Potential Vorticity Diagnostics of Hurricane Movement. Part II: Tropical Storm Ana (1991) and Hurricane Andrew (1992)

CHUN-CHIEH WU*

Program in Atmospheric Sciences, Princeton University, Princeton, New Jersey

KERRY A. EMANUEL

Center for Meteorology and Physical Oceanography, Massachusetts Institute of Technology, Cambridge, Massachusetts

(Manuscript received 30 November 1993, in final form 6 May 1994)

ABSTRACT

The validity of balance dynamics in the Tropics allows an exploration of the dynamics of hurricanes using the potential vorticity (PV) framework. Part I demonstrated the use of PV diagnostics in understanding the hurricane steering flow and also the interaction between the cyclone and its environment. To obtain a broader understanding of this PV methodology, two other observational case studies are performed (Tropical Storm Ana of 1991 and Hurricane Andrew of 1992) emphasizing the same methods of analysis.

The results are consistent with a previous finding that the hurricane advection flow, defined by inverting the entire PV distribution excluding the storm's own positive anomaly, is a good approximation to real cyclone movement, even though the original data cannot capture the actual hurricane strength. This study confirms that upper-level PV anomalies can play an important role in the motion of the storm. But their quantitative effect on the cyclone's motion depends strongly on the relative location of the vortex and the upper-air PV features. Due to the limitations of the data, the β effect or the mechanism proposed by Wu and Emanuel was not able to be supported or disproved.

1. Introduction

A new method for understanding hurricane movement using potential vorticity diagnostics has been presented in Part I (Wu and Emanuel 1995). In particular, Part I analyzed the movement of Hurricane Bob (1991). Part I showed that the new technique is useful in understanding the steering (advection) of storms. By applying the technique of piecewise potential vorticity inversion, the interaction between individual large- and synoptic-scale disturbances and storm movement can be quantitatively evaluated. Since Bob spent most of its lifetime in the middle latitudes along the east coast of the United States, it is not clear whether these previous findings can be generalized. For this reason, we also investigate other storms that differ from each other and from Bob in intensity, size, location, track direction, and track speed. Here we present an analysis of Tropical Storm Ana (1991) and Hurricane Andrew (1992), employing the same method as described in Part I.

The tracks of Tropical Cyclone Ana and Hurricane Andrew are displayed in Fig. 1. As shown in Part I, Hurricane Bob was an intense hurricane that moved mainly to the north and north-northeast along the east coast of United States. By contrast, Ana was a relatively weak tropical storm, originating along the East Coast between Georgia and Florida and then moving east-northeastward. Hurricane Andrew was the strongest of the three cases. Andrew had a relatively small-sized circulation. Unlike Bob and Ana, Andrew spent most of its lifetime south of 30°N, maintaining a more tropical character. Also, Andrew's motion differed from the other two in that it moved generally westward, except turning northward before its final landfall along the south-central Louisiana coast.

We shall use the same climatological mean (using the July–September 1991 time average as the mean fields in all cases and neglecting the possible year-to-year variation) to define the perturbation fields associated with these three cyclones. As in Part I, we use L to represent the lower PV perturbation [300 mb and below (including potential temperature perturbations at 925 mb)] and U for the upper PV perturbation [250 mb and above (including potential temperature perturbations at 125 mb)]. We divide L into two parts: the

* Current affiliation: Department of Atmospheric Sciences, National Taiwan University, Taipei, Taiwan.

Corresponding author address: Dr. Chun-Chieh Wu, Dept. of Atmospheric Sciences, National Taiwan University, 61, Ln 144, Sec 4, Keelung Rd., 10772 Taipei, Taiwan.

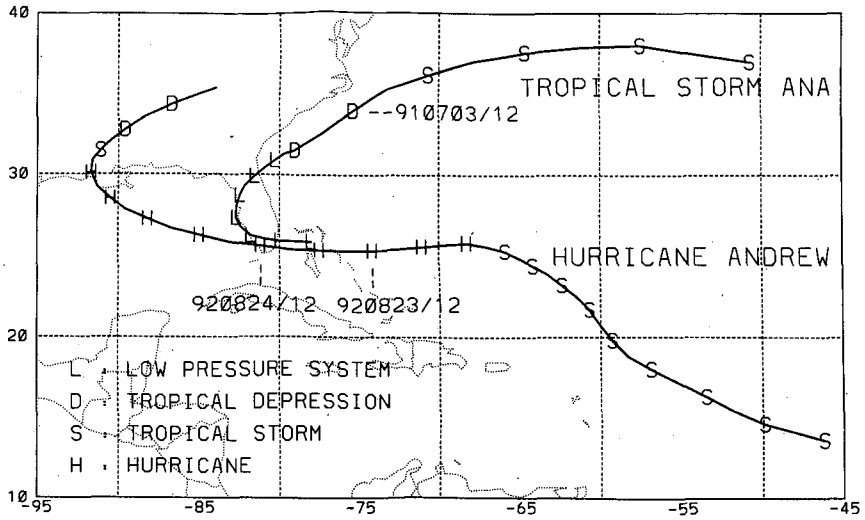

FIG. 1. Best track positions for Tropical Cyclone Ana of 1991 and Hurricane Andrew of 1992. The L, D, S, and H indicate the storm position every 12 h.

lower PV of the tropical storm itself (the positive PV anomalies at 300 mb and below representing the hurricane, denoted as LS) and the remainder (the entire PV anomaly distribution at 300 mb and below, *excluding the hurricane anomaly,* denoted as LE). We will then employ potential vorticity diagnostics to understand the key dynamical processes contributing to the differing track directions and track speeds among the storms. In addition, as in Part I, we define the *hurricane advection flow* as the summation of the balanced flows (interpolated to the storm center) associated with the climatological mean PV, U, and LE.

The analyses of Tropical Storm Ana and Hurricane Andrew are presented in sections 2 and 3. Section 4 summarizes our work.

2. Tropical Storm Ana

a. Synopsis of Ana

Ana was the first tropical storm of the 1991 hurricane season. Its best track positions are shown in Fig. 1. As indicated from the Hurricane Preliminary Report from the National Hurricane Center, Ana originated from a low pressure trough located about 300 miles east of Jacksonville, Florida, on 25 June 1991. The system moved toward the northern Bahamas, and by 1200 UTC 27 June, a small surface low formed. In the next few days, this system moved across southern Florida, curved northward along the west coast of Florida, and then headed northeastward toward the St. Augustine area. At about 1800 UTC 2 July, Ana became a tropical depression about 100 miles south of Charleston, South Carolina.

Moving toward the northeast along the coast of South and North Carolina, Ana gradually intensified, and a weak circulation was found by an air force reconnaissance plane, with 15 m s^{-1} winds at the 457-m (1500 ft) flight level. At 2000 UTC 3 July, Ana was upgraded to a tropical storm by the National Hurricane Center.

Ana then moved east-northeastward, and at 0900 UTC 4 July, a maximum sustained wind of 23 m s^{-1} was reported. Ana continued moving eastward and gradually lost its tropical characteristics by 1800 UTC on the 5th.

b. An example: 1200 UTC 3 July 1991

Seven different times from 0000 UTC 2 July to 0000 UTC 5 July are used for this case study. Specifically, we choose 1200 UTC 3 July as an example for discussion.

At 1200 UTC 3 July, Ana appeared as a local relative vorticity maximum in the lower troposphere, with an amplitude of 4.5×10^{-5} s^{-1} at 700 mb. The amplitude of this vorticity maximum decreased upward and vanished above 300 mb. This can also be found in the PV field (not shown here). Ana had a PV maximum of 0.5 PVU (potential vorticity unit; 10^{-6} m^2 s^{-1} K kg^{-1}) at 850 mb, which increased to about 0.8 PVU at 700 and 500 mb. In the upper troposphere (e.g., at 150 mb), there was a large region of low-PV air to the east of the storm over the western Atlantic. Consistent with the finding in Part I, the PV field here also shows that the PV distribution was uniform in the lower troposphere and that the horizontal PV gradient is much higher in the upper troposphere.

The balanced height and NMC analyzed wind fields at 700 mb indicate that Ana's circulation is partially captured by the analyses. There existed a wavelike flow bending to the south of Ana, with a wind speed of about

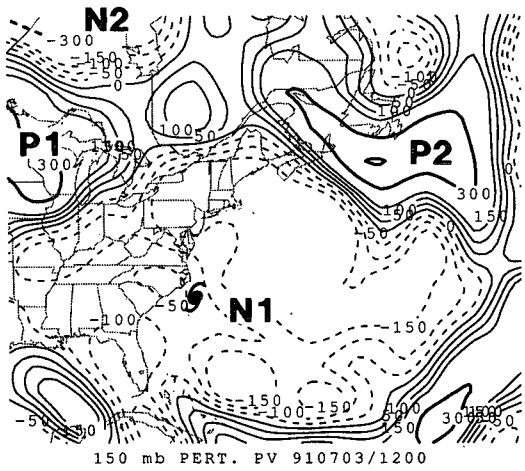

FIG. 2. Ertel's potential vorticity perturbation field at 150 mb at 1200 UTC 3 July 1991. The unit is 0.01 PVU. Potential vorticity values smaller than or equal to (larger than) 1.5 PVU are shown as thin lines (bold lines) with contour intervals of 0.5 PVU (1.5 PVU). Positive (negative) values are represented by solid (dashed) lines. Tropical Storm Ana's best track positions are indicated by the hurricane symbol.

10 m s^{-1}. Again, the NMC analyses cannot resolve the actual strength of Ana.

The 150-mb PV perturbation field is shown in Fig. 2. We define the following individual anomalies: a large-scale negative PV anomaly covering the southeast United States and west Atlantic (referred to as N1), a negative PV anomaly over central Canada (N2), a positive PV anomaly over the northwest-central United States (P1), and a positive PV anomaly located to the south of Newfoundland (P2). Three anomalies, P1, P2, and N2, extended downward to 500 mb. Therefore, the simple partition of PV perturbations into U and L is not optimal in representing these PV anomalies. However, to be consistent with the other cases, we conduct piecewise inversion of some portions of these PV anomalies in the upper four levels and lower six levels, separately.

The 700-mb balanced flow fields associated with each PV perturbation are displayed in Fig. 3. The balanced flow inverted from U (Fig. 3a) includes four main features: two cyclonic gyres associated with the synoptic-scale positive PV anomalies (P1 and P2) and two anticyclonic gyres associated with the large-scale negative PV anomalies (N1 and N2). The saddle point of the four circulations is located near Buffalo, New York. As indicated in Fig. 3a, Ana is located near the center of the southern branch of the anticyclonic circulations, and it appears that Ana's motion is only slightly influenced by the flow associated with U at this time.

Figure 3b shows the 700-mb balanced flow associated with L. A weak circulation surrounding Ana is found. A southerly flow of more than 12 m s^{-1} exists to the east of Ana. The two cyclonic circulations near the central United States and south of Newfoundland are associated with the upper-tropospheric positive PV anomalies that extend down to the middle and lower troposphere. The balanced flow associated with LE (which excludes the positive PV anomaly associated with Ana) is displayed in Fig. 3c. It is similar to that shown in Fig. 3b, except that a uniform southwesterly is found through Ana's center. This southwesterly flow (associated with LE) extends from southwest of Florida to the east coast of North Carolina and contributes to advecting Ana northeastward at 5 m s^{-1}. Our analysis from piecewise PV inversion of individual PV anomalies indicates that this southwesterly flow is a result of the sum of the balanced flows associated with the two positive PV anomalies (extension of P1 and P2 between 700 and 300 mb), a positive PV anomaly near central Mexico, and a negative lower-level PV anomaly to the east and southeast of the storm. Finally, the 700-mb balanced flow (Fig. 3d) associated with Ana's positive PV anomaly (LS) indicates a cyclonic circulation with a maximum wind of 6 m s^{-1}.

The 850–500-mb pressure-weighted average balanced flows associated with each PV perturbation are interpolated to the storm center to represent Ana's advection flow (Figs. 4a,b). Again, we use both the best track center (a) (33.9°N, 75.4°W) and the balanced vortex center (b) (33.17°N, 75.10°W) for interpolation. In this example, these two centers are separated by about 1° latitude. As discussed in Part I, the balanced flows associated with the mean and U are about the same when these different centers are used for interpolation, but the interpolation of the balanced flows of L differs by nearly 2 m s^{-1}. In this example, the advection of Ana is mainly associated with the mean flow and LE. Unlike the case of Bob, due to the cancellation effects between the PV anomalies, the upper-tropospheric disturbances (U) do not have a large effect on Ana's motion at this time.

The sum of the balanced flows associated with the mean climatological PV, U, and LE comprises Ana's total advection flow. As shown in Figs. 4a and 4b, the magnitude of the vector error between the total advection flow and Ana's actual motion, which is northeastward at 11 m s^{-1}, is 1.7 m s^{-1}. The result demonstrates that our definition of advection flow is close to the actual motion of Ana and that the result is not very sensitive to which interpolation center is used.

Figure 4c also shows the advection flow (interpolated to the 850–500-mb pressure-averaged balanced vortex center) at each level. In this example, it appears that the mean vertical shear above Ana is weak. In other words, Ana is advected by a uniform tropospheric flow at its center.

c. Time evolution of Ana

1) EVOLUTION OF UPPER-LEVEL PV ANOMALIES

Figure 5 shows the evolution of the tropopause potential temperature (θ) perturbation field, and Fig. 6

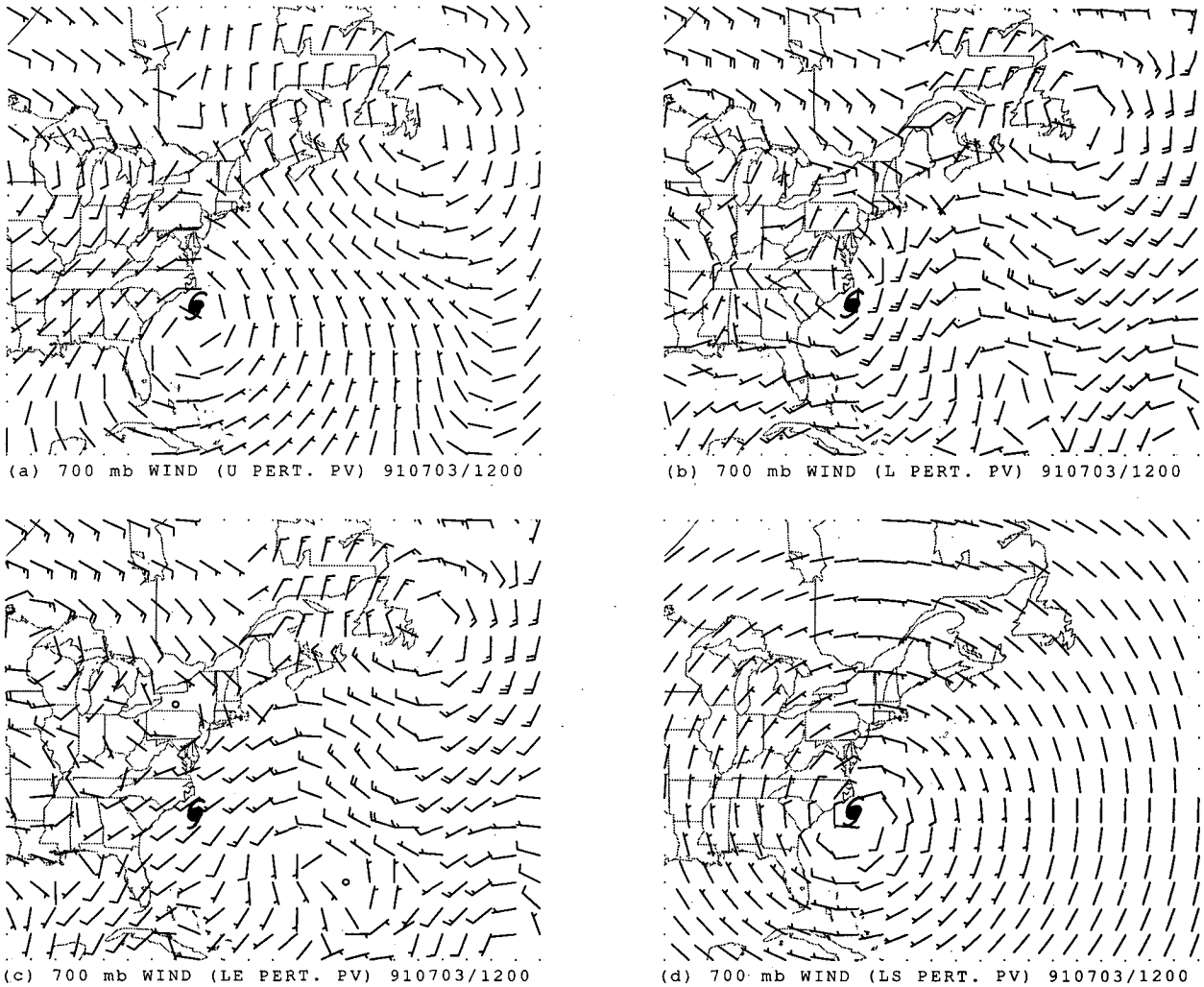

FIG. 3. The 700-mb balanced wind fields (barb with unit in knots) associated with (a) U, (b) L, (c) LE, and (d) LS at 1200 UTC 3 July 1991. One long barb indicates 10 kt (8–12 kt); one short barb indicates 5 kt (3–7 kt); no barb indicates winds less than 3 kt; "0" indicates no wind. Tropical Storm Ana's best track positions are indicated by the hurricane symbol.

displays the evolution of 700-mb balanced flow associated with the upper-four-level PV perturbations (U). At 0000 UTC 2 July, as shown in Fig. 5a, there are three anomalies in the midlatitudes: one cold anomaly (referred to as C1) is located over the west-central United States, another warm anomaly (W1) is over the Great Lakes, and a second cold anomaly (C2) is centered over southern Newfoundland. The balanced flow field at 700 mb is shown in Fig. 6a. There exists a meridionally elongated anticyclonic circulation squeezed between two cyclonic gyres (the gyre at the west side is not located within the domain of Fig. 6a). A west-southwestward flow of 2 m s^{-1} through Ana's center is found and is mainly associated with W1 and partly with C2.

All the anomalies are advected eastward in time by the climatological mean westerlies. Figure 5b shows that, 12 h later, W1 is divided into two parts: the northern portion (W2) over central Canada and the southern portion (W3) centered over New York. The 700-mb balanced flow field (Fig. 6b) is similar to those in Fig. 6a, with a weaker advection flow (1.3 m s^{-1}) for Ana.

At 0000 UTC 3 July, as indicated from Fig. 5c, W3 weakens slightly, extends southeastward, and covers the west Atlantic, but its center of maximum amplitude remains near New York and northern Pennsylvania. Cold anomaly C2 also remains at the same location, with a stronger amplitude than it had 12 h ago. Figure 6c shows that the center of the anticyclonic circulation is farther south relative to W3's center. This is probably due to the deformation by the two gyres of cyclonic flows associated with C1 and C2. At this time, Ana is located slightly to the south of the center of this anti-

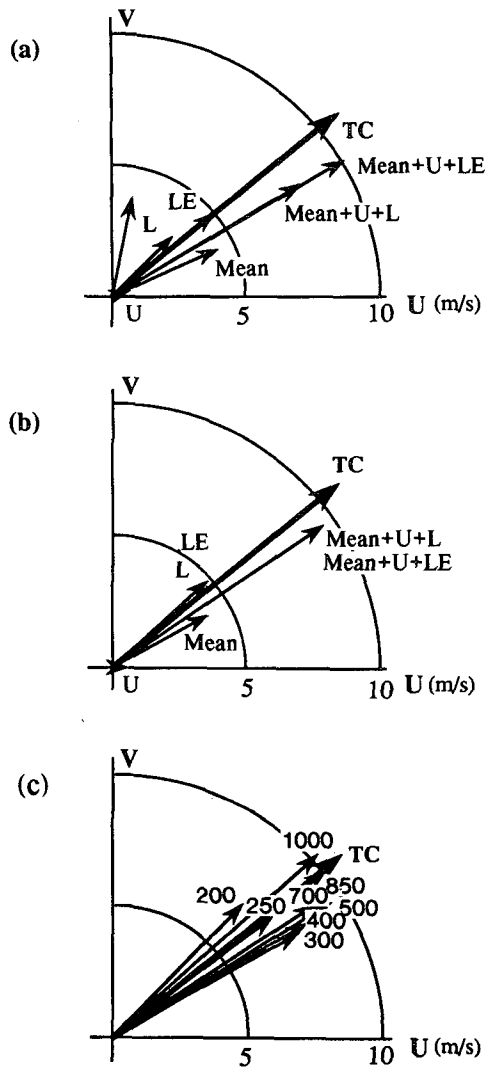

FIG. 4. Velocity vectors of balanced flows and Tropical Storm Ana's motion at 1200 UTC 3 July 1991. Mean, U, L, and LE represent the 850–500-mb pressure-averaged balanced flows associated with the mean potential vorticity and potential vorticity perturbations of U, L, and LE, respectively. Mean + U + LE represents the total hurricane advection flow. TC indicates Ana's motion estimated from every 6-h best track position. Interpolation of the balanced wind fields (a) to the best track center and (b) to the 850–500-mb pressure-averaged balanced vortex center. (c) Velocity vectors of total advection flow (interpolated to the 850–500-mb pressure-averaged balanced vortex center) at each level.

cyclonic circulation and is advected by a northeasterly of 1.1 m s^{-1}.

Twelve hours later, as shown in Fig. 5d, all systems move slightly toward the east; only C2's center remains at the same position with weaker intensity. In the meantime, another warm anomaly (W4) forms over the south-central United States. As was discussed previously, the balanced flow field (Fig. 6d) is primarily composed of circulations associated with C1, C2, W2, W3, and W4. Also, there exists a rather weak westerly (0.5 m s^{-1}) that advects Ana, as Ana is located slightly to the north of the anticyclonic circulation center.

At 0000 UTC 4 July, as shown in Fig. 5e, W3 covers a broad area over the west Atlantic, and W4 is located at the southeast United States. The 700-mb balanced flow (Fig. 6e) looks similar to that of 12 h ago (Fig. 6d). The anticyclonic circulation to the southeast of North Carolina has an eastward advection effect (1.6 m s^{-1}) on Ana.

Twelve hours later, the potential temperature field (Fig. 5f) remains about the same as that in Fig. 5e, except that W4 strengthened and shifted slightly northeastward. The inverted balanced flow at 700 mb (Fig. 6f) has an anticyclonic circulation more zonally elongated over the west Atlantic. It has a contribution of 2.7 m s^{-1} to Ana's eastward movement.

At 0000 UTC 5 July, as shown in Fig. 5g, W3 extends farther to the east. A region of high θ (a portion of W4) is found to the east of North Carolina. At this time, Ana is located between W3, W4, and C2, and a stronger balanced flow (Fig. 6g) between these PV anomalies advects Ana southeastward at 4.5 m s^{-1}.

Overall, this case study shows how upper-level disturbances influence a storm's motion, depending on the distribution and amplitude of these disturbances. It should also be noted that following the evolution of the tropopause θ information in Fig. 5, we do not observe any kind of warm anomaly (upper negative PV anomaly) that is unambiguously related to Ana. In contrast to Bob's analyses, there is no clear signature of the generation of negative PV anomaly aloft of Ana, perhaps because Ana is too weak to be revealed in the data. For comparison, we also look at the evolution of the 200-mb streamlines analyzed by the National Hurricane Center. It appears that there are only a few observations over the area near Ana, and these do not show an anticyclonic flow field over Ana.

2) EVOLUTION OF LOWER- AND MIDDLE-LEVEL PV ANOMALIES

The comparison of the analyzed wind and relative vorticity field with the actual best track maximum sustained speed (not shown) demonstrates that the NMC analyses do not correctly represent the actual evolution of Ana's strength.

The evolution of the 700-mb PV perturbation fields (not shown) indicates that Ana appeared as a positive PV anomaly with an amplitude of 0.2 PVU at 0000 UTC on the 2d. It increased to about 0.3 PVU at 1200 UTC 3 July. This PV anomaly weakened to 0.2 PVU on the 4th, but intensified to 0.4 PVU at 0000 UTC on the 5th. Following the evolution of 700-mb PV fields, we do not see clear evidence of β gyres near the storm.

As in Part I, the evolution of the 700-mb balanced flow associated with LE is also studied, and the contribution of each individual anomaly to Ana's motion

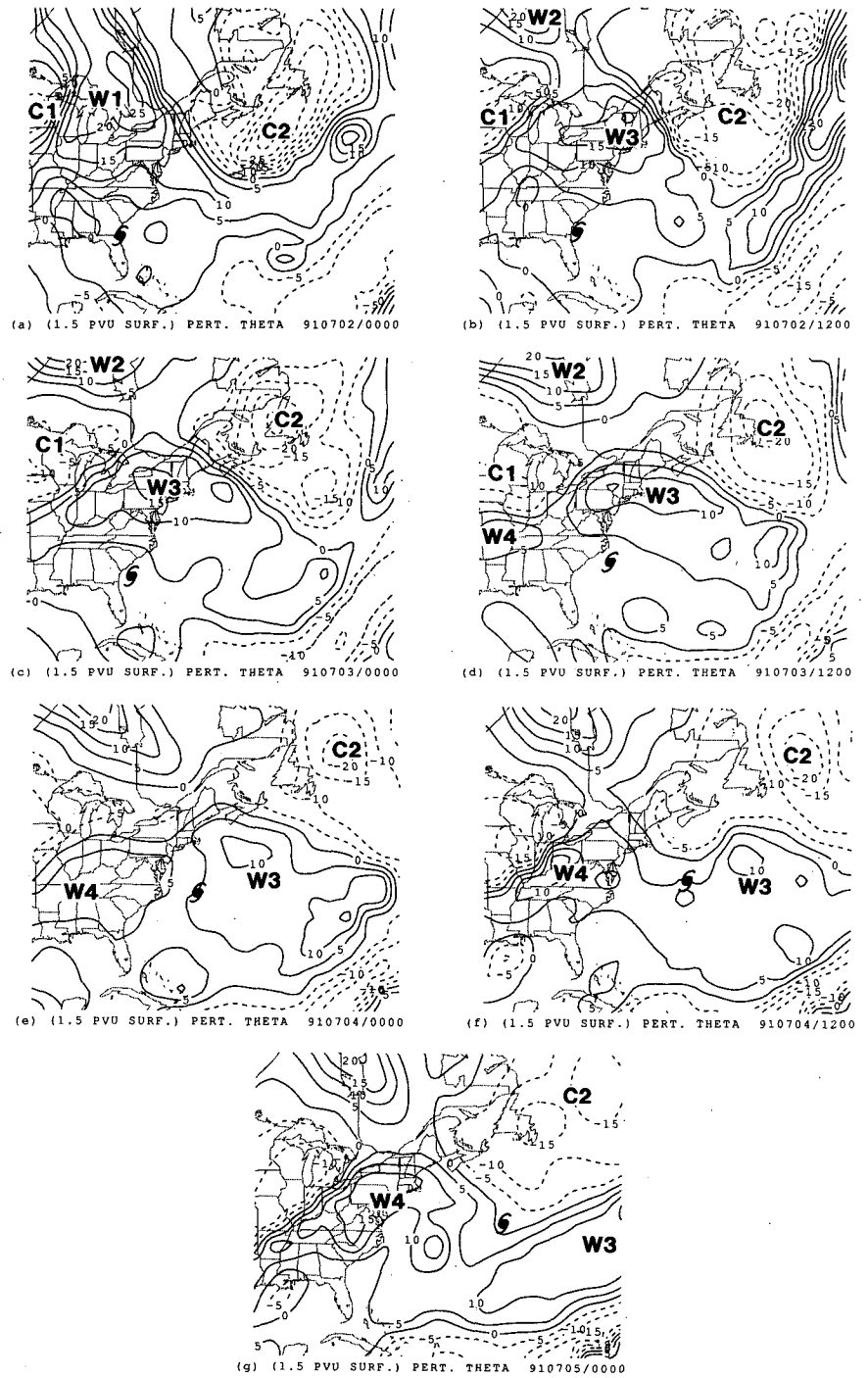

FIG. 5. Time evolution of the tropopause potential temperature perturbation field (on the 1.5-PVU surface) from 0000 UTC 2 to 0000 UTC 5 July 1991. (a) 0000 UTC 2, (b) 1200 UTC 2, (c) 0000 UTC 3, (d) 1200 UTC 3, (e) 0000 UTC 4, (f) 1200 UTC 4, and (g) 0000 UTC 5 July 1991. The contour interval is 5 K. All positive (negative) values are represented by solid (dashed) lines. Tropical Storm Ana's best track positions are indicated by the hurricane symbol.

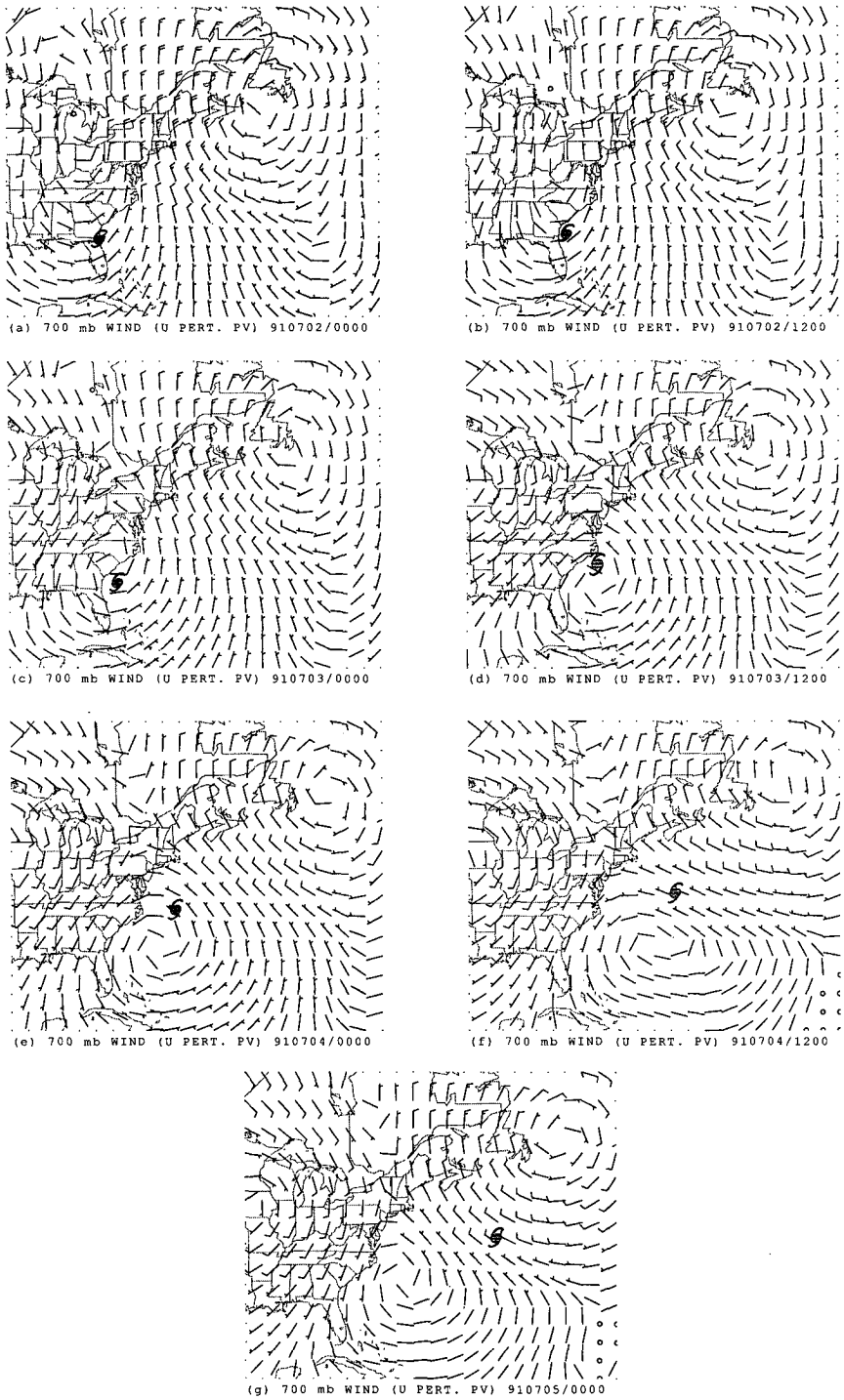

FIG. 6. Time evolution of the 700-mb balanced wind field (wind barb plotted as in Fig. 3) associated with U from 0000 UTC 2 to 0000 UTC 5 July 1991. (a) 0000 UTC 2, (b) 1200 UTC 2, (c) 0000 UTC 3, (d) 1200 UTC 3, (e) 0000 UTC 4, (f) 1200 UTC 4, and (g) 0000 UTC 5 July 1991. Tropical Storm Ana's best track positions are indicated by the hurricane symbol.

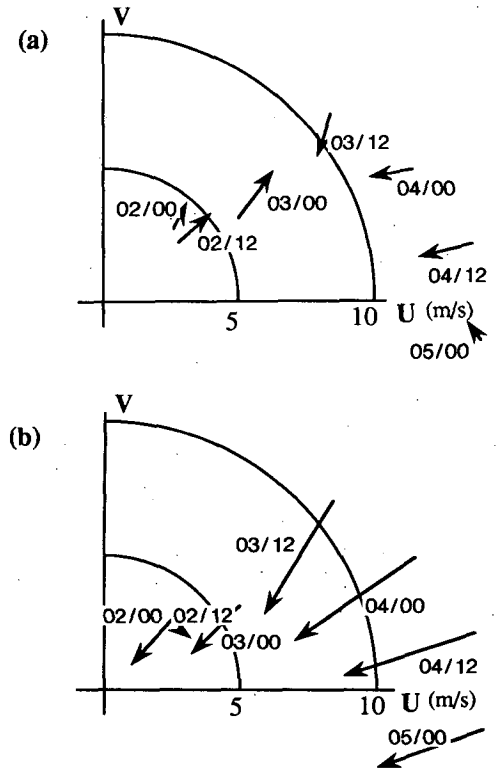

FIG. 7. (a) Velocity vector differences between the 850–500-mb pressure-averaged advection flow (interpolated to the 850–500-mb pressure-averaged balanced vortex center) and Ana's motion from 0000 UTC 2 to 0000 UTC 5 July 1991. (b) Velocity vector differences between the 850–500-mb pressure-averaged annular mean flow and Ana's motion.

is identified (not discussed here). In this example, LE plays an important role in advecting Ana.

d. Advection flow of Ana

Figure 7a displays the hodographs that demonstrate the velocity vector differences between the 850–500-mb pressure-averaged advection flow (interpolated to the 850–500-mb averaged balanced vortex center) and Ana's actual movement from 0000 UTC 2 July to 5 July. The advection flow approximates Ana's motion well. In the seven different times, the mean magnitude of the vector errors is 1.5 m s^{-1}, with a standard deviation of 0.7 m s^{-1}. This case study indicates that the advection flow derived from our PV diagnostics is particularly good in representing the direction of Ana's movement, though the advection speed differs about 10%–20% from the real cyclone displacement velocity.

We also calculate the velocity differences (Fig. 7b) between the mean flow calculated over an annulus 5°–7° from the centers, as defined in Part I, and the storm's actual motion. The differences are much larger than those shown in Fig. 7a. In Fig. 7a, the vectors appear to point in random directions. However, there appears to be some consistent southwestward bias of the annular mean flows in Fig. 7b. The statistics from the seven different times show that the average magnitude of the vector differences is 3.7 m s^{-1} with a standard deviation of 1.8 m s^{-1}. This result indicates that the annular mean may represent a flow field that has no direct relation with the advection flow at the storm center. This finding again shows that our method is capable of detecting the storm's advection current while, using the same NMC gridded datasets, the approximate annular mean flow appears to be biased.

3. Hurricane Andrew

a. Synopsis of Andrew

Andrew was the first and the strongest Atlantic tropical cyclone of the 1992 hurricane season. As seen from Andrew's best track positions (Fig. 1), it had a long lifetime of nearly 2 weeks from 16–28 August. Andrew was a compact and ferocious hurricane that originated over the tropical North Atlantic Ocean, then moved westward across the northwestern Bahamas and the southern Florida peninsula, and made its final landfall in south-central Louisiana.

Andrew formed from a tropical wave over Africa and then moved out over the tropical North Atlantic Ocean on 14 August. It became a tropical depression at around 1800 UTC 16 August. The depression became stronger as the environmental vertical wind shear diminished. At 1200 UTC 17 August, it was upgraded to Tropical Storm Andrew. Then Andrew moved northwestward with its central pressure rising slightly on the following 3 days.

Andrew intensified again on 21 August as it turned and accelerated toward the west and became a hurricane on the morning of 22 August. In the meantime, Andrew's eye formed. Andrew intensified dramatically in the next 36 h and reached its peak intensity at 1800 UTC 23 August, with a central pressure of 922 mb and a maximum wind speed of 69 m s^{-1}.

Andrew maintained its westward movement, passing over northern Eleuthera Island late on the 23d and then over the southern Berry Islands early on the 24th. After crossing through the Straits of Florida, it made landfall east of Homestead Air Force Base at 0900 UTC 24 August and then passed over the southern portion of the Florida peninsula in about 4 h.

As Andrew reached the Gulf of Mexico, it gradually turned toward the west-northwest and slowed down. Andrew made its final landfall near the south-central Louisiana coast at 0830 UTC 26 August and weakened rapidly as it moved inland.

b. Examples: 1200 UTC 23 and 24 August 1992

Eight different times from 1200 UTC 19 to 1200 UTC 26 August 1992 (only 1200 UTC are used) are

analyzed. We choose two particular times (1200 UTC 23 and 24 August) to show the general behavior of Andrew from the NMC datasets.

At 1200 UTC 23 August, a few hours before it reached its maximum strength, Andrew was located about 400 miles east of Miami. The analyses indicate a local relative (potential) vorticity maximum with an amplitude of 4.7×10^{-5} s^{-1} (0.5 PVU). This vorticity maximum extended from 850 to 300 mb. At 150 mb, a region of negative relative vorticity and local PV minimums is observed to the north-northeast of Andrew.

The balanced height and NMC analyzed wind fields at 700 mb show that there existed a weak cyclonic circulation, with an azimuthal wind speed of only about 6 m s^{-1}, surrounding Andrew. The NMC analyses, while locating Andrew correctly, far underestimated its strength. Compared to Bob, the NMC analyses are worse in capturing Andrew's intensity possibly because of its small size.

At 1200 UTC 24 August, Andrew was located at the southwest portion of the Florida peninsula, with an analyzed intensity much stronger than 24 h before. As indicated from the relative vorticity and PV fields, at this time, Andrew had a local relative (potential) vorticity maximum of 9.4×10^{-5} s^{-1} (1.0 PVU). This vorticity maximum extended from 850 to 300 mb. At 150 mb, a strong local PV minimum was found above and to the east of Andrew.

The NMC analyzed wind speed around Andrew increased to 14 m s^{-1}. However, other models, such as the NGM, show a wind maximum of about 30 m s^{-1} near 850 mb at the same time. Comparing the NMC analyses at 1200 UTC the 23d and the 24th, the NMC data analyze Andrew much better at the latter time, when Andrew was located in Florida rather than over the ocean.

Andrew was a positive PV anomaly in the lower and middle troposphere, with an amplitude of 0.25 PVU, which is about the same strength as Tropical Storm Ana. At 150 mb (Fig. 8), a negative PV anomaly of −1.5 PVU is found above and to the northeast of Andrew. In addition, a distinct positive PV anomaly (denoted as P3) existed over southeast Nova Scotia and extended downward to about 500 mb. Also, a negative PV anomaly (referred to N3) existed over the north-central United States and central Canada and was confined to above 400 mb. At 500 and 700 mb, a negative PV anomaly of −0.5 PVU is found over and to the north of the Gulf of St. Lawrence.

The 700-mb balanced flow fields associated with each PV perturbation are displayed in Fig. 9. The balanced flow associated with U (Fig. 9a) is dominated by the dipole gyres associated with the two aforementioned distinct PV anomalies, P3 and N3. These circulations are nearly opposite to those indicated in Bob at 1200 UTC 18 August 1991. The flow advects Andrew toward the south-southwest at 2.1 m s^{-1}. The balanced flow associated with L (Fig. 9b) features a cyclonic circulation surrounding Andrew with a wind speed of about 10 m s^{-1}. However, when we invert LE (excluding Andrew's PV anomaly), the 700-mb balanced flow field (Fig. 9c) shows a distinct anticyclonic circulation associated with the middle-tropospheric negative PV anomaly over the Gulf of St. Lawrence. This clockwise circulation extends southward into the subtropics and combines with a uniform east-northeasterly that passes through Andrew's center with a speed of 4 m s^{-1}. Figure 9d shows the 700-mb balanced flow associated with Andrew's PV anomaly (LS). The maximum wind speed associated with Andrew itself is only 5 m s^{-1} in this analysis.

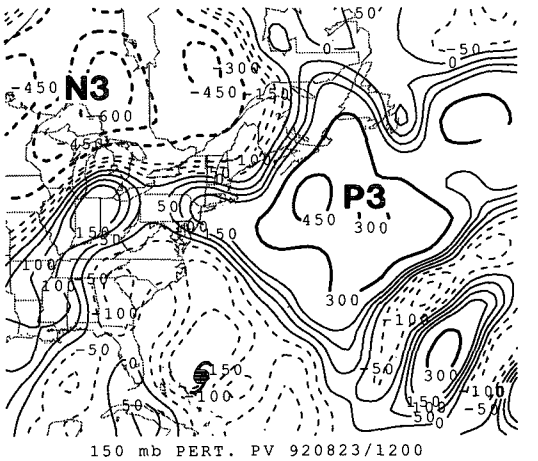

FIG. 8. Ertel's potential vorticity perturbation field at 150 mb at 1200 UTC 23 August 1992. The unit is 0.01 PVU. Potential vorticity values smaller than or equal to (larger than) 1.5 PVU are shown as thin lines (bold lines) with contour intervals of 0.5 PVU (1.5 PVU). Positive (negative) values are represented by solid (dashed) lines. Hurricane Andrew's best track positions are indicated by the hurricane symbol.

Figure 10a shows the comparison of the advection flow (averaged between 850 and 500 mb and interpolated to the balanced vortex center) with Andrew's actual motion at 1200 UTC 23 August. In this example, the balanced vortex center differs from the best track position by about 0.7° latitude. The climatological mean, U, and LE have about the same magnitude of contribution to Andrew's advection flow. The magnitude of the vector difference between the advection flow and Andrew's motion, which is 7.7 m s^{-1} westward, is 1.7 m s^{-1}. The advection flow at each level is also displayed in Fig. 10b. In this example, an east-northeasterly vertical wind shear of 8 m s^{-1} between 200 and 700 mb over Andrew is found. Andrew's motion appears to correlate better with the lower- to midtropospheric advection flow than the upper-level flow.

The positive PV anomaly of Andrew increases to 0.4 PVU at 700 mb at 1200 UTC 24 August, which is about two times the amplitude of Andrew's PV anomaly on

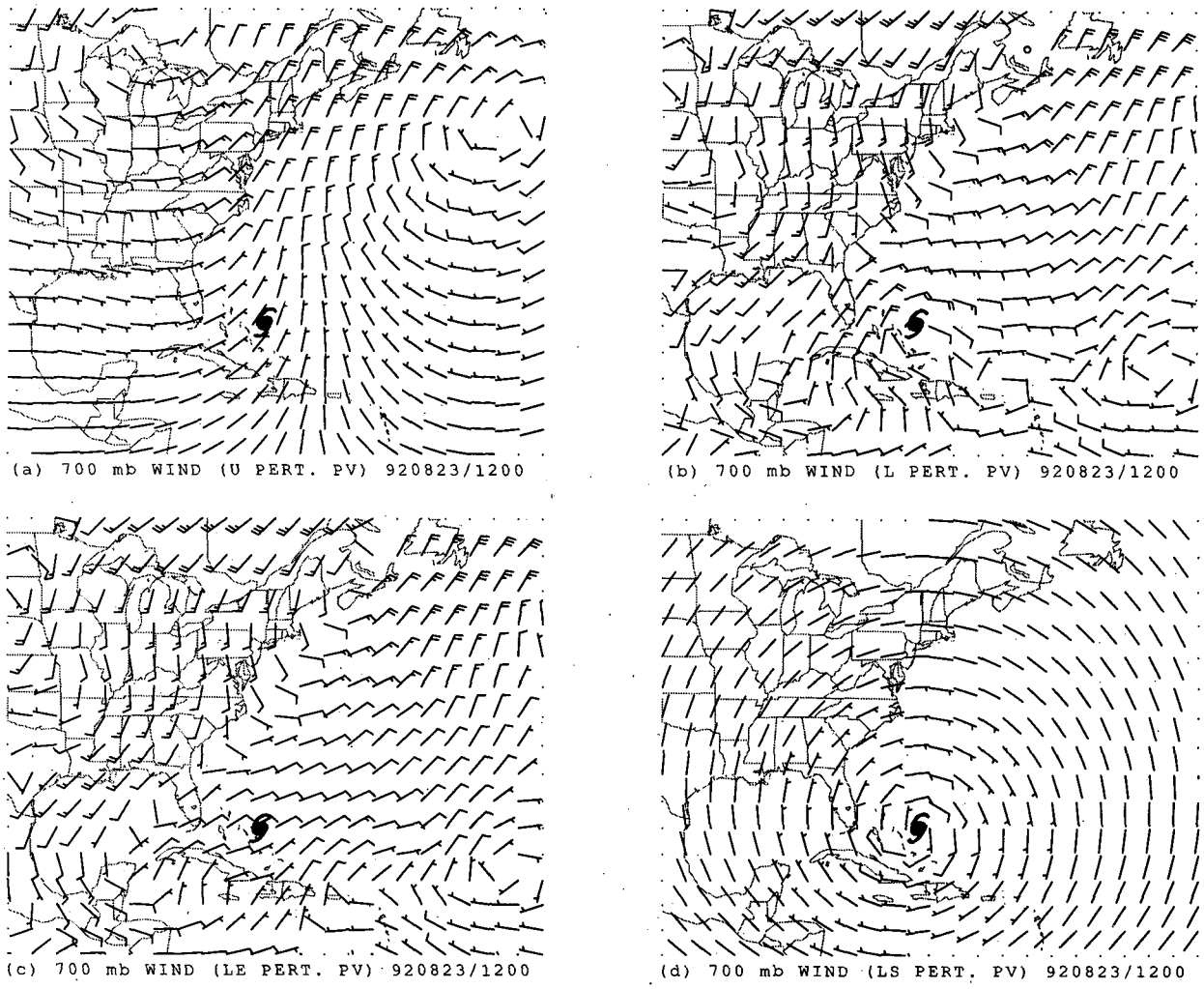

FIG. 9. The 700-mb balanced wind fields (wind barb plotted as in Fig. 3) associated with (a) U, (b) L, (c) LE, and (d) LS at 1200 UTC 23 August 1992. Hurricane Andrew's best track positions are indicated by the hurricane symbol.

the 23d. At 150 mb (Fig. 11), a negative PV anomaly of −1.5 PVU is found above Andrew. Also, at this time, P3 moves southeastward and stretches in a southwest–northeast orientation over the northwest Atlantic Ocean. The negative PV anomaly N3 moves eastward with its PV maximum above central Canada. The mid-level negative PV anomaly, located near the Gulf of St. Lawrence on the 23d, extends farther south.

The 700-mb balanced flow fields associated with each PV perturbation are displayed in Fig. 12. The balanced flow associated with U (Fig. 12a) is dominated by the dipole gyres associated with P3 and N3. Compared with the balanced flow 24 h ago, the dipole gyres are seen to interact with each other, having a tendency to move southwestward together and become stronger. A southwestward flow with a speed of 3.1 m s^{-1} is found at Andrew's center. The balanced flow associated with L (Fig. 12b) indicates a cyclonic circulation surrounding Andrew with a wind speed of about 13 m s^{-1}. However, when we invert LE (excluding Andrew's PV anomaly), the balanced flow field at 700 mb (Fig. 12c) shows an easterly wind of 4.5 m s^{-1} through Andrew's center. Figure 12d shows the 700-mb balanced flow associated with Andrew's PV anomaly (LS). The maximum wind speed associated with Andrew itself is 9 m s^{-1} in this analysis.

The comparison of the 850–500-mb pressure-averaged advection flow and Andrew's motion at 1200 UTC 24 August is displayed in Fig. 13a. The balanced flow associated with U and LE is equally important in contributing to Andrew's advection flow. Again, the advection flow is a good approximation to Andrew's movement, which is 8.9 m s^{-1} westward. The magni-

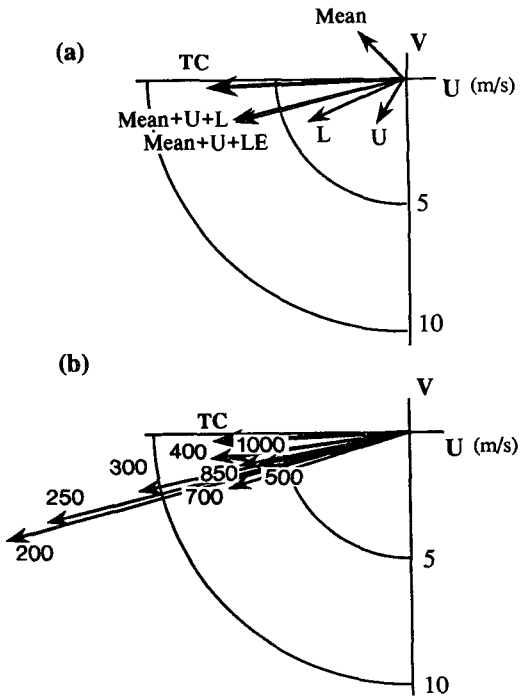

FIG. 10. (a) Velocity vectors of balanced flows (interpolated to the 850–500-mb pressure-averaged balanced vortex center) and Hurricane Andrew's motion at 1200 UTC 23 August 1992. Mean, U, L, and LE represent the 850–500-mb pressure-averaged balanced flows associated with the mean potential vorticity and potential vorticity perturbations of U, L, and LE, respectively. Mean + U + LE represents the total hurricane advection flow. TC indicates Andrew's motion estimated from every 6-h best track position. (b) Velocity vectors of total advection flow at each level.

tude of the vector difference between the total advection flow and Andrew's motion is 1.6 m s^{-1}. The advection flow at each level is also illustrated in Fig. 13b. In this example, an easterly vertical wind shear of 5 m s^{-1} between 200 and 700 mb is found over Andrew. The result also shows that the lower- and midtropospheric (1000–400 mb) advection flow has the best correlation with Andrew's actual motion.

c. *Time evolution of Andrew*

In this section, we discuss the evolution of the PV features in both the upper and lower-middle troposphere. The evolution of the balanced flow fields associated with these PV anomalies, and their influence of Andrew's movement are also examined. Since Andrew has a relatively long lifetime, we choose a 24-h interval, from 1200 UTC on the 19th to 1200 UTC on the 26th, for this evolution study.

1) EVOLUTION OF UPPER-LEVEL PV ANOMALIES

Figure 14 shows the evolution of the potential temperature θ field on the dynamic tropopause (1.5-PVU surface) from 1200 UTC 19 to 26 August. Also, Fig. 15 displays the evolution of the 700-mb balanced flow inverted from the upper-four-level PV perturbation U.

At 1200 UTC 19 August, as shown in Fig. 14a, a warm anomaly (referred to as W5) is located to the east of Newfoundland. The central and eastern United States is covered by a broad cold anomaly, with one maximum (C3) over the Great Lakes and the other (C4) near the border of Oklahoma and Texas. In the meantime, an area of warm anomaly is present to the east above Andrew. It is not clear whether this is directly related to Andrew. The projection of the flow associated with U at 700 mb (Fig. 15a) is dominated by two dipole circulations associated with W5, C3, and C4. A weak northward flow of 0.8 m s^{-1} through Andrew's center is found. One day later, C3, C4, and W5 all move southeastward (Fig. 14b), and are still the main upper-level PV features that dominate the 700-mb flow field (Fig. 15b). Another weak warm anomaly (W6) is present at the southwest coast of the United States. The northward advection flow over Andrew associated with U increases slightly to a value of 1 m s^{-1}.

On the 21st, as shown in Fig. 14c, W5 moves to the eastern boundary of the domain, and C3 shifts eastward, centered to the south of Newfoundland. Meanwhile, a small-amplitude warm anomaly (W7) exists to the north-northeast of the Caribbean. The balanced flow (Fig. 15c) that influences Andrew's motion is dominated by a southwesterly wind of 1.4 m s^{-1} between the two counterrotating circulations associated with C3, C4, and W7.

Figure 14d indicates that on the 22d, another warm anomaly (W8) enters the western boundary of the do-

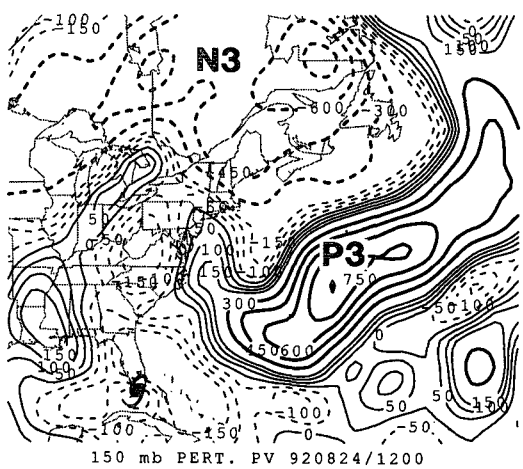

FIG. 11. Ertel's potential vorticity perturbation field at 150 mb at 1200 UTC 24 August 1992. The unit is 0.01 PVU. Potential vorticity values smaller than or equal to (larger than) 1.5 PVU are shown as thin lines (bold lines) with contour intervals of 0.5 PVU (1.5 PVU). Positive (negative) values are represented by solid (dashed) lines. Hurricane Andrew's best track positions are indicated by the hurricane symbol.

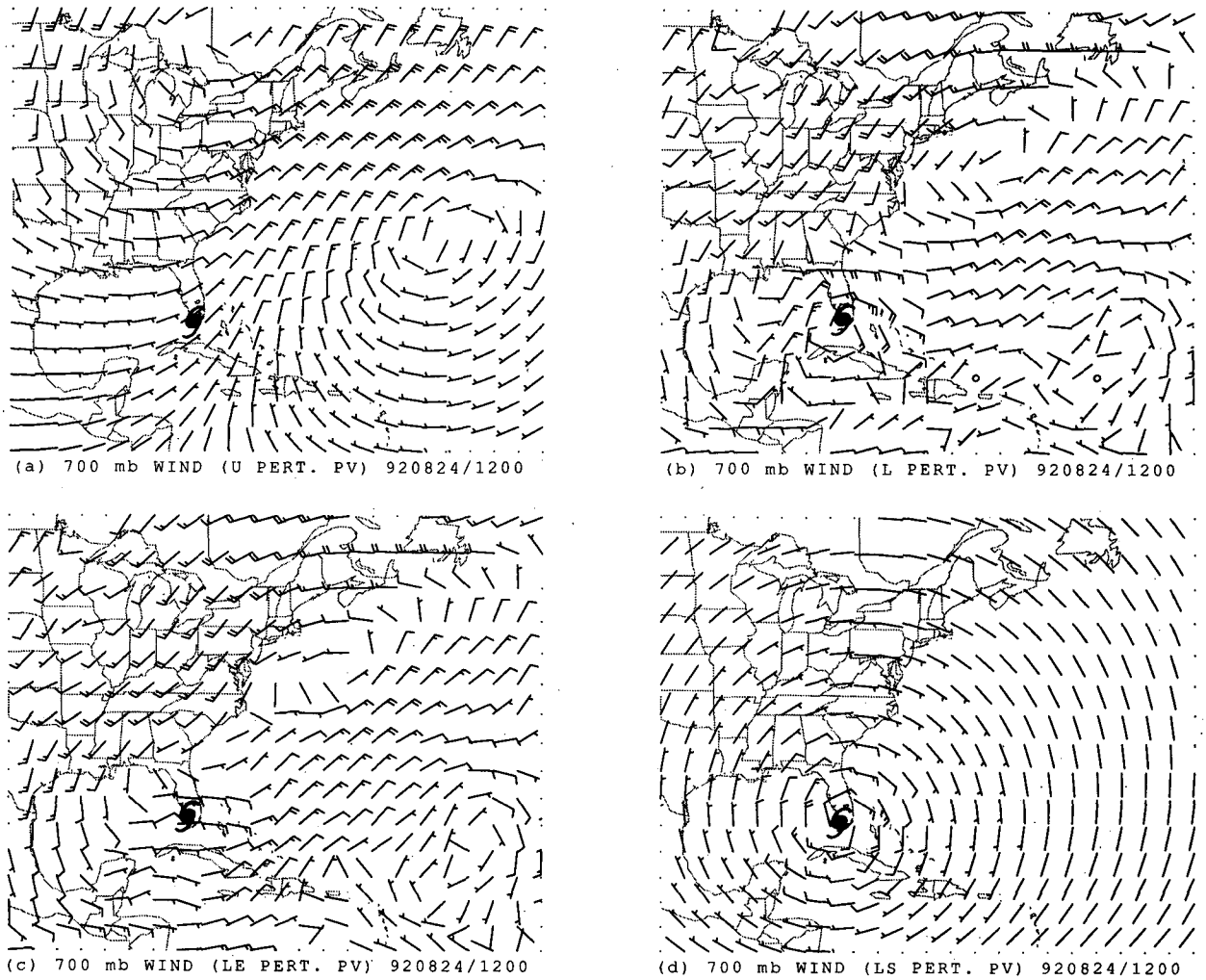

FIG. 12. The 700-mb balanced wind fields (wind barb plotted as in Fig. 3) associated with (a) U, (b) L, (c) LE, and (d) LS at 1200 UTC 24 August 1992. Hurricane Andrew's best track positions are indicated by the hurricane symbol.

main, extending from California to Minnesota, and has an amplitude of 20 K. The balanced flow at 700 mb (Fig. 15d) is different from that 12 h ago. It is dominated by the gyres associated with C3, W6, and W8. The circulation of C4 is countered by the flow associated with W6 and W8. At this time, the effect of U on Andrew's motion has changed: it advects Andrew southward by a weak flow of 0.7 m s^{-1}. This is also the time when Andrew changed direction from northwestward to westward.

On the 23d, as shown in Fig. 14e, both W8 and C3 intensify and are the dominant dynamic features in the upper troposphere. Warm anomaly W8 extends from Arizona to Quebec, and C3 is located to the southeast of Newfoundland over the northwest Atlantic Ocean. C4 is still confined to a narrow band, centered over Louisiana. The projection of U at 700 mb is a pair of counterrotating circulations (Fig. 15e) that advected Andrew southwestward at 2.1 m s^{-1}.

On the 23d, a small-scale warm anomaly of 5 K is located to the east above Andrew. However, just 1 day later, as displayed in Fig. 14f, a distinct warm anomaly of 20 K forms over Andrew. The timing of the occurrence of this θ (or PV) anomaly above Andrew matches well with the time when the NMC analyses better capture Andrew's strength. Therefore, this warm anomaly is a clear indication of the diabatic generation of the upper-level negative PV anomaly by Andrew, which is not resolved in the NMC data in Andrew's early stage.

Figure 14f also shows that on the 24th, the leading edge of W8 expands over Newfoundland, and C3 is stretched farther southward to the west Atlantic. The balanced flow (Fig. 15f) indicates a stronger wind be-

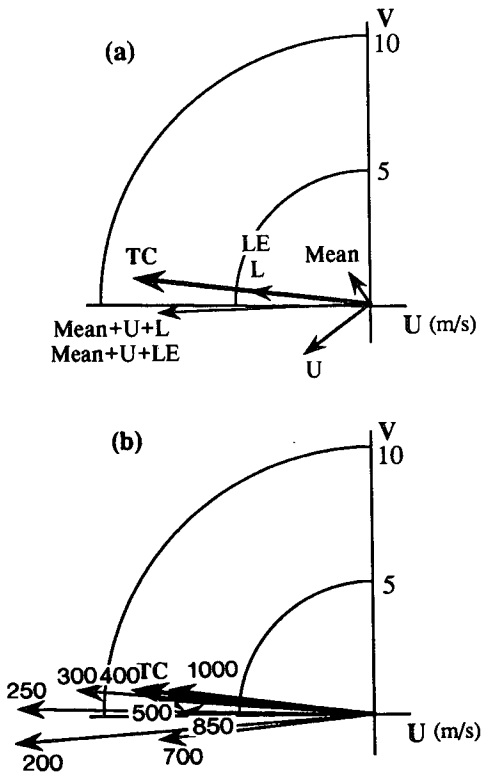

FIG. 13. (a) Velocity vectors of balanced flows (interpolated to the 850–500-mb pressure-averaged balanced vortex center) and Hurricane Andrew's motion at 1200 UTC 24 August 1992. Mean, U, L, and LE represent the 850–500-mb pressure-averaged balanced flows associated with the mean potential vorticity and potential vorticity perturbations of U, L, and LE, respectively. Mean + U + LE represents the total hurricane advection flow. TC indicates Andrew's motion estimated from every 6-h best track position. (b) Velocity vectors of total advection flow at each level.

tween the two circulations that advects Andrew southwestward with a speed of 3.2 m s^{-1}.

On 25 August, Fig. 14g indicates a warm anomaly above Andrew, though its amplitude is 10 K weaker than 1 day earlier. Meanwhile, W8 moves slightly to the east and C3 is divided into two pieces: one moves out of the eastern boundary of the domain and the other stays to the northeast of the Caribbean Islands. The 700-mb balanced flow (Fig. 15g) includes two primary circulations associated with C3 and W8. Andrew's motion due to the influence of upper PV perturbations consists mainly of the balanced flow associated with C3 and W8, which is an easterly wind of 3.5 m s^{-1}.

On the 26th, right after Andrew made landfall in south-central Louisiana, a warm anomaly (Fig. 14h) of 20 K is observed to the southeast and southwest of Andrew. At this time, C3 and W8 both shift slightly eastward. The balanced wind pattern at 700 mb (Fig. 15h) shows that U advects Andrew toward the north-northwest at 2.1 m s^{-1}.

To test the hypothesis advanced by Wu and Emanuel (1993, hereafter WEM), we need to invert the high-θ (low PV) anomaly above Andrew. However, unlike in the case of Bob, as indicated in the previous discussion of the evolution of the PV field, the NMC analyses are not consistent in representing Andrew's intensity and the generation of the low PV anomaly above Andrew. Therefore, we are not sure which part of the negative PV anomaly above Andrew is directly related to it. Also, we do not think the data are able to provide a reliable result that can be used to compare with WEM's numerical model.

For comparison, we look at the evolution of the 200-mb streamlines analyzed by the National Hurricane Center. They are few observations available over the area near Andrew, and these analyses do not show any clear signature of upper anticyclonic flow over Andrew until it reaches the Gulf of Mexico. This result indicates that our objective in examining the effect of upper negative PV anomalies may be limited by the lack of observations over the oceanic region.

2) EVOLUTION OF LOWER AND MIDDLE-LEVEL PV ANOMALIES

The evolution of the relative vorticity field is analyzed from the NMC datasets, from 1200 UTC 19 to 26 August. Comparing the evolution of Andrew's analyzed wind and relative vorticity fields with its best track maximum wind speed (not shown), we find that the NMC analyses do not capture the tendency of Andrew's intensity change. It appears that NMC analyses tend to pick up the storm's intensity better while the storm is over land. Similar results are also found by studying the evolution of the PV fields. Thus, the NMC analyses of Andrew are clearly influenced by how close the storm is to an observation point.

The time evolution of the PV perturbation fields and the balanced flows associated with LE at 700 mb (not shown here) has also been studied. We are able to identify the lower-tropospheric PV features that are most dominant in affecting Andrew's motion. However, following the evolution of the PV anomalies, as in the previous case (Ana), we do not observe any clear signature of β gyres near Andrew.

d. Advection flow of Andrew

Figure 16a shows the hodograph that demonstrates the velocity vector differences between the 850–500-mb pressure-averaged advection flow (interpolated to the 850–500-mb averaged balanced vortex center) and Andrew's actual movement from 1200 UTC 19 to 26 August. In general, the advection flow approximates Andrew's motion well, though a consistent southward component in vector differences is found. At the eight different times, the mean magnitude of the vector differences is 1.9 m s^{-1}, with a standard deviation of 0.7 m s^{-1}. This case study indicates that the advection flow derived from our PV diagnostics is capable of capturing

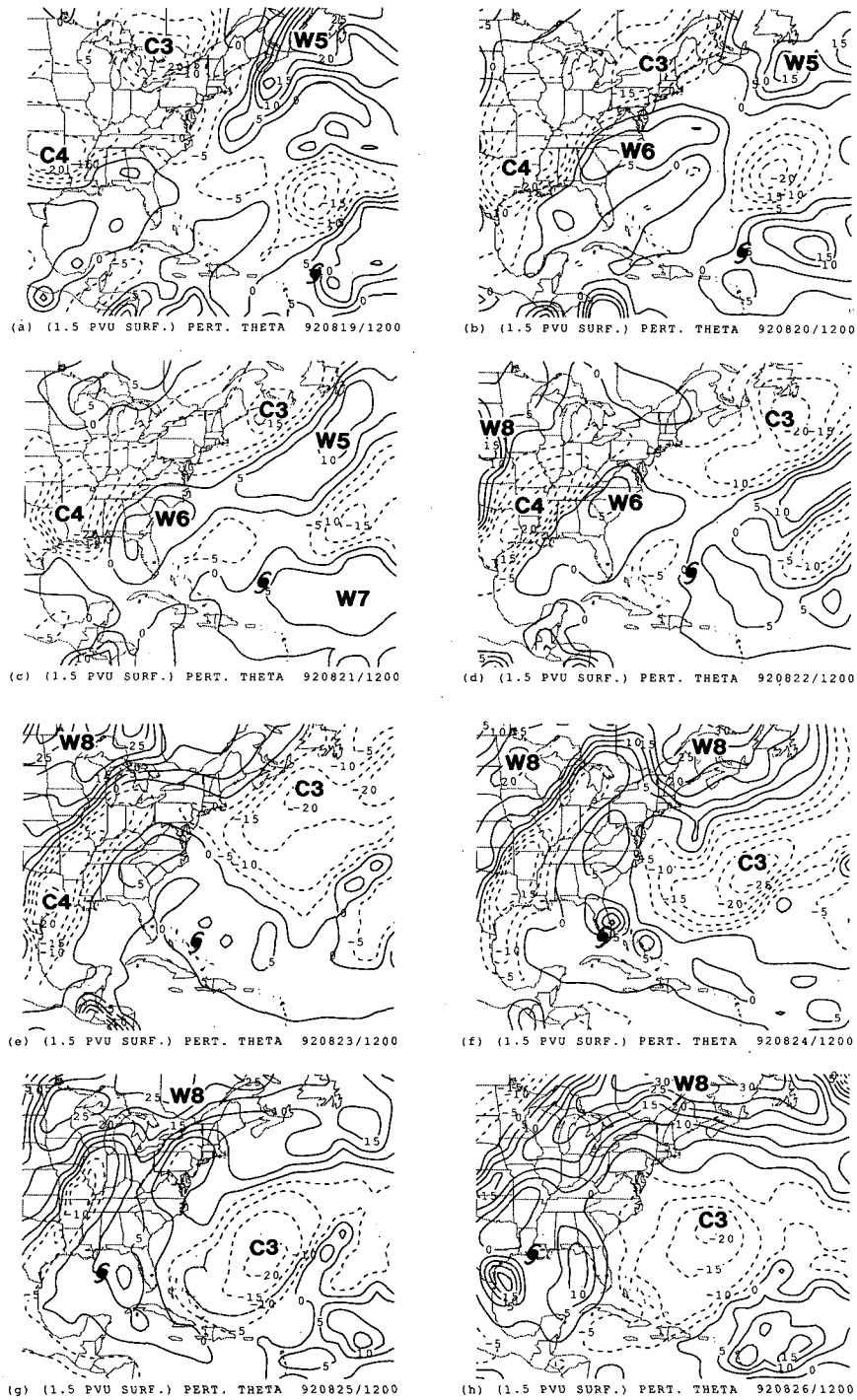

FIG. 14. Time evolution of the tropopause potential temperature perturbation field (on the 1.5-PVU surface) from 1200 UTC 19 to 26 August 1992. (a) 1200 UTC 19, (b) 1200 UTC 20, (c) 1200 UTC 21, (d) 1200 UTC 22, (e) 1200 UTC 23, (f) 1200 UTC 24, (g) 1200 UTC 25, and (h) 1200 UTC 26 August 1992. The contour interval is 5 K. All positive (negative) values are represented by solid (dashed) lines. Hurricane Andrew's best track positions are indicated by the hurricane symbol.

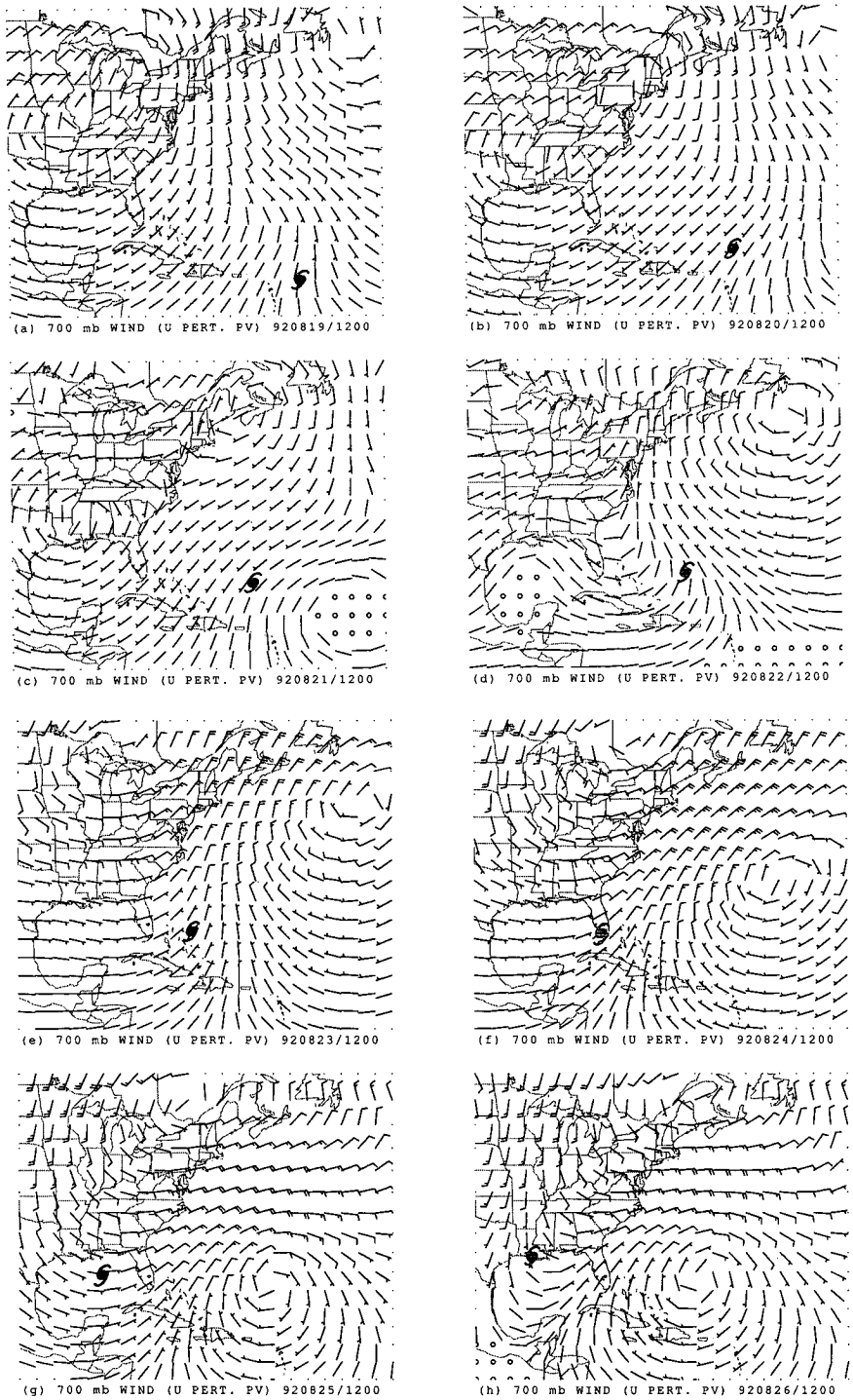

FIG. 15. Time evolution of the 700-mb balanced wind field (wind barb plotted as in Fig. 3) associated with U from 1200 UTC 19 to 26 August 1992. (a) 1200 UTC 19, (b) 1200 UTC 20, (c) 1200 UTC 21, (d) 1200 UTC 22, (e) 1200 UTC 23, (f) 1200 UTC 24, (g) 1200 UTC 25, and (h) 1200 UTC 26 August 1992. Hurricane Andrew's best track positions are indicated by the hurricane symbol.

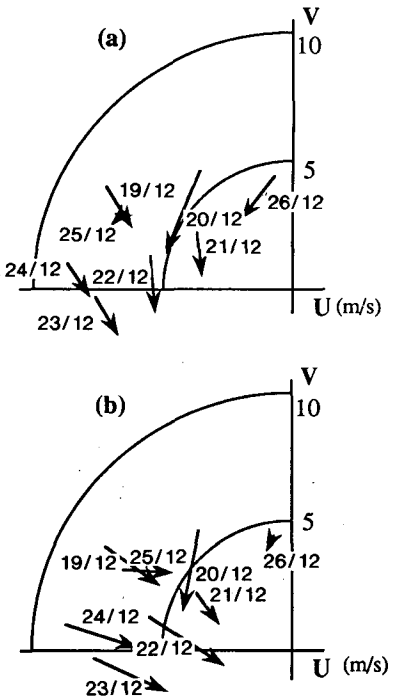

FIG. 16. (a) Velocity vector differences between the 850–500-mb pressure-averaged advection flow (interpolated to the 850–500-mb pressure-averaged balanced vortex center) and Andrew's motion from 1200 UTC 19 to 1200 UTC 26 August 1992. (b) Velocity vector differences between the 850–500-mb pressure-averaged annular mean flow and Andrew's motion.

some of Andrew's movement, though the advection flow appears to be consistently biased toward the south.

We are not sure what causes this systematic southward bias of the advection flow, which is not observed in the other two cases. We speculate that there are two possible reasons for this: first, the southern boundary condition may affect the meridional component of the balanced flow and, second, there may be some important PV features that are not resolved or poorly placed by the NMC analyses, which might have advected Andrew northward.

We also calculate the velocity vector differences (Fig. 16b) between the annular mean flow (as defined in Part I) and Andrew's actual motion. The magnitudes of these differences are larger than those shown in Fig. 16a, and also have a consistent southward bias. The statistics from the eight different times show that the average magnitude of the vector errors is 2.5 m s^{-1} with a standard deviation of 0.9 m s^{-1}. Though not as significant as the other two cases, the advection flow derived from the potential vorticity diagnostics is still a better approximation to the best tracks of Andrew.

4. Summary

In both Part I and this paper, we use the NMC gridded datasets to examine three tropical cyclones using PV diagnostics. Our goal is to understand how the large-scale flow and the hurricane interact with each other. We also investigate the different mechanisms responsible for the storm movement that are described by the traditional theory, which holds that advection of a background PV gradient dominates the influence of the storm on its environment, as by the hypothesis advanced by WEM, which regards the storm-generated plume of low PV near the tropopause as the dominant effect.

Using the seasonal climatology as the mean reference state, piecewise potential vorticity inversions are performed under the nonlinear balance condition. This allows one to determine the balanced flow associated with any individual perturbation of PV. By examining the balanced flow at the hurricane center, one can identify which PV perturbation has the most influence on hurricane movement.

We also define the hurricane advection flow as the balanced flow (at the center of the storm) associated with the whole PV in the troposphere, except for the storm's own positive PV anomaly. Although the NMC analyses have a relatively coarse resolution and cannot capture the actual strength of hurricanes, the results show that such an advection flow is a very good approximation to the real storm motion.

However, in this study, we do not find enough evidence to support the so-called β effect and the effect of the upper negative PV anomaly generated by the storm. It appears that the study of these two effects is strongly compromised by the limitations of the NMC data. For example, the NMC analyses may have too a coarse resolution to resolve the β gyres, and the upper negative PV anomaly diabatically generated by the hurricane over oceans may not be well detected from the raw observations and thus may be underestimated or lost in the NMC analyses. Also it should be remembered that the analyzed flow fields may have errors that are comparable to the signals of these effects (e.g., 2 m s^{-1}), which makes the evaluation of the individual influence of these dynamical processes on hurricane motion even more difficult.

It is emphasized that the advection flow we define is dynamically meaningful, since it is consistent with the concept that hurricanes, at the first order of approximation, are steered by the environmental flow at their centers. The essence of this work is that, using PV diagnostics, we can get a clear picture of how the large-scale flow interacts with the storm. We believe that more insights into the dynamics of hurricane movement can be obtained by applying this PV methodology to better datasets or numerical model output that have a higher resolution and can better represent the hurricane's circulation.

The methodology developed here also suggests a means of "bogusing" tropical cyclones into numerical weather prediction models. Namely, the large potential vorticity anomaly directly associated with the hurricane

is removed in the manner illustrated in this paper. This hurricane PV distribution is then reinserted at the appropriate location indicated by satellite imagery, aerial reconnaisance, and so on, and the new, full PV distribution is then inverted to recover winds, pressure, and temperature. The moisture anomaly directly associated with the hurricane should be relocated in a similar manner. This is a dynamically consistent way of relocating the essential features of the storm without altering the fundamental characteristics of the large-scale ambient atmosphere.

Acknowledgments. This work represents a portion of the first author's Ph.D. dissertation at the Massachusetts Institute of Technology. The authors would like to thank Dr. Christopher Davis for his kind help with the inversion code. The authors also thank Dr. Roger Smith and an anonymous reviewer for their helpful comments. The first author gratefully acknowledges Drs. John Marshall, Glenn Flierl, and Alan Plumb for their valuable suggestions during the course of this work, and Dr. Yoshio Kurihara at GFDL for his support in writing this paper. Credit is also given to Mr. J. Varanyak at GFDL for drafting assistance. This research is supported through the National Science Foundation by Grant ATM-9019615.

REFERENCES

Wu, C.-C., 1993: Understanding hurricane movement from a potential vorticity perspective: A numerical model and an observational study. Ph.D. dissertation, Massachusetts Institute of Technology, 278 pp. [Available from author at Dept. of Atmospheric Sciences, National Taiwan University, 61, Ln 144, Sec 4, Keelung Rd., 10772 Taipei, Taiwan.]

——, and K. A. Emanuel, 1993: Interaction of a baroclinic vortex with background shear: Application to hurricane movement. *J. Atmos. Sci.*, **50**, 62–76.

——, and ——, 1995: Potential vorticity diagnostics of hurricane movement. Part I: A cases study of Hurricane Bob (1991). *Mon. Wea. Rev.*, **123**, 69–92.